Chinese J. Chem. Eng., 13 (3) 350 – 354 (2005)

Crystal Growth Models of Dexamethasone Sodium Phosphate in a MSMPR Reactive Crystallizer

HAO Hongxun(郝红勋)*, WANG Jingkang(王静康), WANG Yongli(王永莉) and HOU Baohong(侯宝红)
School of Chemical Engineering and Technology, Tianjin University, Tianjin 300072, China

Abstract The reactive crystallization process of dexamethasone sodium phosphate was investigated in a continuous mixed-suspension, mixed-product-removal(MSMPR) crystallizer. Analyzing experimental data, it was found that the growth of product crystal was size-dependent. The Bransom, CR, ASL, MJ2 and MJ3 size-dependent growth models were discussed in details. Using experimental steady state population density data of dexamethasone sodium phosphate, parameters of five size-dependent growth models were determined by the method of non-linear least-squares. By comparison of experimental population density and linear growth rate data with those obtained from the five size-dependent growth models, it was found that the MJ3 model predicts the growth more accurately than do the other four models. Based on the theory of population balance, the crystal nucleation and growth rate equations of dexamethasone sodium phosphate were determined by non-linear regression method. The effects of different operation parameters such as supersaturation, magma density and temperature on the quality of product crystal were also discussed, and the optimal operation conditions were derived.
Keywords dexamethasone sodium phosphate, growth model, crystal size distribution(CSD), population balance equation

1 INTRODUCTION

For simulation, design and analysis of industrial crystallizers, experimentally determined and statistically correlated nucleation and growth rates are needed[1−3]. The mixed-suspension, mixed-product-removal(MSM PR) crystallizer can be used for the simultaneous determination of crystal growth and nucleation rates using a population balance analysis of the crystal size distribution(CSD). In the analysis of such MSMPR crystallizer data, non-linearity in semi-log population density-crystal size plots is often observed. The main cause of such curvature seems to be the size-dependent growth or particle agglomeration. In this case, the estimation of kinetics of both nucleation and growth rate becomes more complicated. One way of carrying out the modeling is to adopt a size-dependent growth function such that an "effective" crystal growth model can be determined for the purpose of design. The occurrence of such anomaly of growth rate is reflected in the CSD from the MSMPR crystallizer[4].

As one kind of anti-inflammatory drug of ardrenal cortex hormone, dexamethasone sodium phosphate is widely used in clinical application. In industrial manufacture, dexamethasone sodium phosphate is crystallized from the solution in the purification step. However,it seems that no one has studied its crystal growth and nucleation. The purpose of this paper is to study the crystal growth of dexamethasone sodium phosphate in a continuous MSMPR reactive crystallizer and finally determine its growth and nucleation rate functions which are necessary for design and analysis of industrial crystallizer.

2 THEORY

To a well mixed steady-state MSMPR crystallizer with clear liquor feed, where the particle size only changes owing to crystal growth (*i.e.* both agglomeration and disruption are neglected) and where the CSD and magma density of particles in the product outflow is the same as in the crystallizer, the differential number balance[5] can be expressed in terms of population density $n(L)$ by

$$\frac{\mathrm{d}[G(L)n(L)]}{\mathrm{d}L} + \frac{n(L)}{\tau} = 0 \tag{1}$$

where $G(L)$ is the crystal growth rate, $n(L)$ is the population density, L is the crystal size and τ is the mean residence time of suspension in the crystallizer.

If the McCabe ΔL law holds, the crystal growth rate is size-independent and the solution of Eq. (1) is the well-known MSMPR distribution[6]

$$n(L) = n^0 \exp\left(-\frac{L}{G\tau}\right) \tag{2}$$

In this case, a semi-log plot of population density versus crystal size should therefore give a straight line with slope $-1/G\tau$, from which the crystal growth rate may be determined. The zero-size nucleation rate B^0

Received 2004-05-17, accepted 2004-09-16.
* To whom correspondence should be addressed. E-mail: hhx73@hotmail.com

can be determined as

$$B^0 = Gn^0 \tag{3}$$

where n^0 is the intercept of population density distribution plot at $L = 0$.

If the crystal growth does not obey McCabe ΔL law and the growth rate depends on the size of a growing crystal, the population density distribution will not follow the simple exponential relationship given by Eq. (2). A solution to Eq. (1) then requires information describing the dependence of growth rate on crystal size.

The relationship between crystal size and growth rate has been studied theoretically by a number of authors and many different size-dependent growth rate models have been proposed. Some typical models which are widely used in research work can be summarized as follows.

Bransom model[7]

$$G(L) = aL^b \tag{4}$$

Canning-Randolph(CR) model[8]

$$G(L) = G_0(1 + aL) \tag{5}$$

Mydlarz and Jones(MJ2) model[9]

$$G(L) = G_m[1 - \exp(-aL)] \tag{6}$$

Abegg, Stevens and Larson(ASL) model[10]

$$G(L) = G_0(1 + aL)^b \tag{7}$$

Rojkowski exponential model[11]

$$G(L) = G_1 - (G_1 - G_0)\exp(-aL) \tag{8}$$

Rojkowski hyperbolic model[12]

$$G(L) = \frac{G_0 + aG_1L}{1 + aL} \tag{9}$$

Mydlarz and Jones(MJ3) model[13]

$$G(L) = G_m\{1 - \exp[-a(L + c)]\} \tag{10}$$

In these models, it has been showed recently that Rojkowski exponential model can be written in a form similar to the MJ3 model[14]. The Rojkowski hyperbolic model is not suitable for introducing the influence of temperature and supersaturation on crystal growth rate. So in this paper, only the other five models were discussed.

By combining with the five size-dependent growth models, the population balance equation can be integrated to give the following.

Bransom model

$$n(L) = n^*\exp\left[\frac{1}{a\tau(b-1)}(L^{1-b} - L^{*1-b}) - \ln\left(\frac{L}{L^*}\right)^b\right] \tag{11}$$

Canning-Randolph(CR) model

$$n(L) = n^0(1 + aL)(-1 - a\tau G_0)/a\tau G_0 \tag{12}$$

Mydlarz and Jones(MJ2) model

$$n(L) = n^*\exp[a(L - L^*)]\left[\frac{\exp(aL) - 1}{\exp(aL^*) - 1}\right]^{(-1-b)/b} \tag{13}$$

Abegg, Stevens and Larson (ASL) model

$$n(L) = n^0(1 + aL)^{-b}\exp\left[\frac{1}{1-b} - \frac{(1 + aL)^{1-b}}{1-b}\right]$$
$$\tau G_0 = a^{-1} \tag{14}$$

Mydlarz and Jones (MJ3) model

$$n(L) = K\exp(aL)[A\exp(aL) - 1]^{(-1-b)/b}$$
$$K = n^0(A - 1)^{(1+b)/b}$$
$$A = \exp(ac)$$
$$B = a\tau G_m \tag{15}$$

where a, b, c are the growth model parameters, G_0 is the zero-size crystal growth rate, G_1 and G_m are the limiting growth rates of large crystals, L^* is the chosen crystal size.

3 EXPERIMENTAL

The experimental apparatus and procedure used in this study are shown in Fig. 1. The reactive crystallization processes were carried out in an continuous MSMPR crystallizer. The crystallizer geometric configuration is shown in Fig. 1. The supersaturation was produced by the reaction of dexamethasone phosphate with sodium hydroxide solution. The reaction mixture was mechanically agitated using an four-blade pitch-type impeller which located at the center of crystallizer. The impeller rotation speeds were maintained at $330\,r\cdot min^{-1}$. Temperature control within the crystallizer was achieved by pumping constant temperature water continuously through the hollow draft tube at the maximum possible rate. The temperature difference between the solution and the constant temperature water was about 0.1°C and in this way the crystallizer temperature in all runs was controlled to within ±0.1℃. In experiments, all solvents and other chemical materials used were purchased and had a purity higher than 99.5%. The flowrate of each solution was kept constant during the steady state experiment so as to keep the mean residence time constant. The suspension density varies

from 10.28 kg·m^{-3} to 30.15 kg·m^{-3}. Malvern Mastersizer(MAM5005) by Malvern Instruments Limited was used to measure the crystal size distribution(CSD) of dexamethasone sodium phosphate which was sampled after the crystallization process reached the steady state.

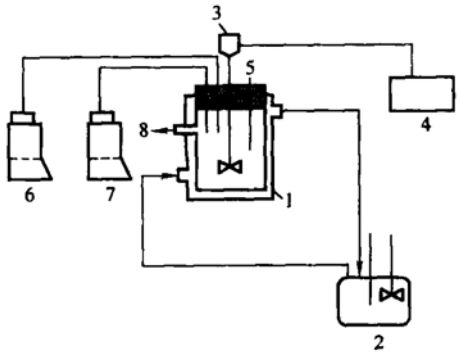

Figure 1 Schematic diagram of experimental apparatus
1—MSMPR crystallizer; 2—super thermostat; 3—stirrer; 4—stirrer controller; 5—thermometer; 6, 7—liquid pump; 8—liquid outlet

4 RESULTS AND DISCUSSION

The semi-log population density versus crystal size plot for dexamethasone sodium phosphate obtained from a continuous MSMPR crystallizer in a typical reactive crystallization experiment is depicted in Fig. 2.

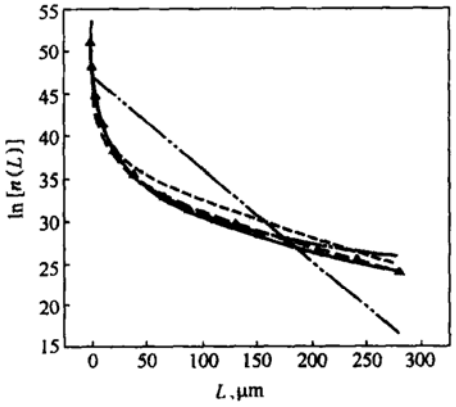

Figure 2 Comparison of experimental population density data with those calculated by different size-dependent growth models
—— Bransom; -·-·- CR; -·-·- ASL; - - - - MJ2; – – – MJ3; ▲ Experiment

It can be noted from Fig. 2 that the semi-log population density data of dexamethasone sodium phosphate exhibit curvature, particularly in the small size range(0—100 μm). This shows that the growth of dexamethasone sodium phosphate violates McCabe ΔL law and the size-independent growth rate model is not appropriate for describing the crystal growth in reactive crystallization processes.

The main cause of exhibiting curvature phenomenon as shown in Fig. 2 may be due to the size-dependent growth or particle agglomeration. The SEM photographs of dexamethasone sodium phosphate obtained by reactive crystallization were shown in Fig. 3. From Fig. 3, it can be seen that the agglomeration phenomenon can be neglected in reactive crystallization of dexamethasone sodium phosphate. So, the size-dependent growth was considered. Five size-dependent growth rate models were used to describe the growth of dexamethasone sodium phosphate in reactive crystallization. In order to evaluate the applicability of the five size-dependent growth rate models, the experimental data presented in Fig. 2 were fitted with the five size-dependent steady-state population density distribution Eqs. (11)—(15) respectively. Values of model parameters calculated with non-linear regression are presented in Table 1.

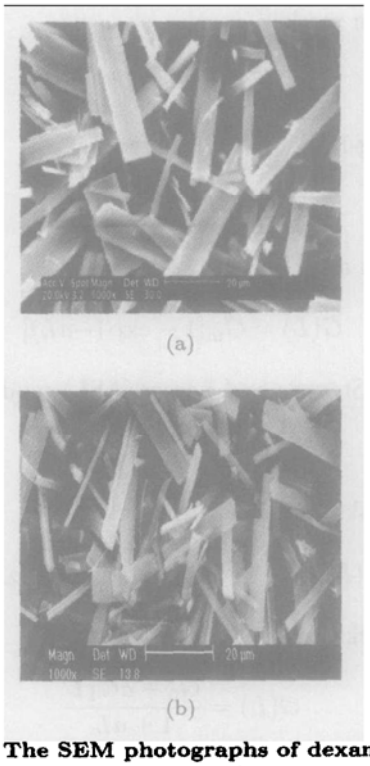

Figure 3 The SEM photographs of dexamethasone sodium phosphate

Using those data listed in Table 1, the fits of the five theoretical population density distribution curves are also shown in Fig. 2. It can be seen that the population density Eq. (12) by CR model does not reproduce the experimental data well, moreover, the other four population density equations, especially Eqs. (13) and (15) by MJ2 and MJ3 models, reproduce the original experimental data reasonably well respectively, throughout the entire size range. This indicates that MJ2 and MJ3 steady-state distribution functions are more appropriate to predict the population density distribution of dexamethasone sodium phosphate.

Table 1 Kinetic constants of empirical size-dependent growth rate models

Model	Equation	Model parameters						
		$a \times 10^{-4}$ m^{-1}	b	$c \times 10^{8}$ m	$G_0 \times 10^{9}$ $m \cdot s^{-1}$	$G_m \times 10^{9}$ $m \cdot s^{-1}$	$B^0 \times 10^{-13}$ $s^{-1} \cdot m^{-3}$	$n^0 \times 10^{-20}$ $no \cdot m^{-1} \cdot m^{-3}$
Bransom	$G(L) = aL^b$	7.172×10^{-6} $m^{1-b} s^{-1}$	0.783	—	—	—	—	—
Canning-Randolph	$G(L) = G_0(1 + aL)$	-20.56×10^{4}	—	—	2.328	—	—	3.03
ASL	$G(L) = G_0(1 + aL)^b$	130.9	4.743		0.1931		4.472	2320
MJ2	$G(L) = G_m[1 - \exp(-aL)]$	2.297	0.560	—	—	6.167	—	—
MJ3	$G(L) = G_m\{1 - \exp[-a(L + c)]\}$	1.586	0.450	6.3	—	7.167	—	26900

It is interesting to compare the growth rates estimated by the five size-dependent growth rate models using parameters listed in Table 1 with experimental data. The result is presented in Fig. 4. It should be pointed out that in the crystal size range of 0—100 μm the difference between growth rates predicted by all five models and experimental values is small. For the larger crystals, however, the MJ3 model fits the experimental growth rate data much better than the other four models. It should also be pointed out that using the Bransom, C-R and ASL models, the growth rates $G(L)$ tend monotonically to infinity in the larger size range, as shown in Fig.4. This is physically unrealistic. The MJ3 size-dependent growth model, on the other hand, approaches asymptotically a maximum growth rate which is consistent with the value of G_m obtained from the slope of population density plot for larger crystal. Furthermore, the Bransom and MJ2 models can not predict zero-size crystal growth rate. So, the Bransom, CR, ASL and MJ2 models are thus not very successful in representing the observed size-dependent growth rates of dexamethasone sodium phosphate. The MJ3 size-dependent growth rate model can predict the growth rate of dexamethasone sodium phosphate well throughout the entire size range.

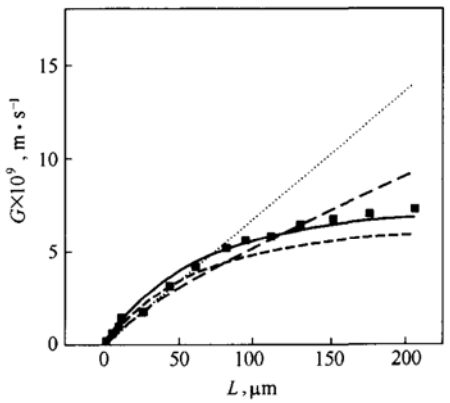

Figure 4 Comparison of experimental linear growth rates with those derived with different size-dependent growth models

■ Experiment; – – – Bransom; - - - - CR; ····· MJ2; —— MJ3

It can be concluded from above that the MJ3 crystal growth model can accurately describe the growth of dexamethasone sodium phosphate in reactive crystallization processes.

Using MJ3 size-dependent growth model and series of experimental population density data obtained in different experimental operation conditions(temperature, initial concentration, magma density and supersaturation), the crystal growth and nucleation rate equations of dexamethasone sodium phosphate in reactive crystallization processes can be determined by non-linear least-square method as follows

$$B^0 = 2.765 \times 10^{20} \exp(-5.196 \times 10^4 / RT) \cdot \Delta C^{1.65} M_T^{2.84} \tag{16}$$

$$G = 4.232 \times 10^4 \exp(-5.628 \times 10^4 / RT) \cdot \Delta C^{0.75} \cdot \{1 - \exp[-1.586 \times 10^4 (L + 6.300 \times 10^{-8})]\} \tag{17}$$

where ΔC is supersaturation, M_T is magma density, T is absolute temperature.

The mean square error S_y of Eq. (16) and Eq. (17) are 6.33% and 8.68% respectively. The calculation equation for S_y can be expressed as

$$S_y = ((\sum((X_i - X_c)/X_i)^2)/n)^{0.5} \tag{18}$$

where X_i is the experimental values of G or B^0, X_c is the calculated value of G or B^0 and n is the number of experimental points.

From Eqs. (16) and (17), it can be seen that the exponential rates of crystal growth and nucleation to supersaturation are 1.65 and 0.75 respectively. This shows that both the crystal growth and nucleation rates increase with the increase of supersaturation, but the nucleation rate increases more rapidly. So increasing the supersaturation is not favorable to obtain crystals with larger size. It also can be seen that the increase of growth rate of dexamethasone sodium phosphate is slightly faster than that of nucleation rate by increasing the crystallization temperature. The growth rate is independent of suspension

density; the nucleation rate increases slowly with the increase of magma density. So, high crystallization temperature, low magma density and supersaturation will benefit to get dexamethaseon sodium phosphate crystals of larger size.

5 CONCLUSIONS

The major emphasis of this paper has been to study the growth model of dexamethasone sodium phosphate in reactive crystallization. A continuous MSMPR crystallizer was used to measure crystal size distribution. It was found that the experimental semi-log population density distribution data exhibit curvature which shows that the size-independent growth rate model is not appropriate for describing the growth of dexamethasone sodium phosphate. Five size-dependent growth rate models were used to predict the steady-state population density distribution and growth rate of dexamethasone sodium phosphate. By comparison, it was found that the MJ3 size-dependent growth model can predict the crystal growth of dexamethasone sodium phosphate more accurately than do the other four models. Application of the MJ3 size-dependent growth model to the experimental population density data under different conditions resulted in the growth and nucleation rate functions of dexamethasone sodium phosphate in reactive crystallization process to be determined. Through analysis of these functions, it was found that supersaturation, temperature and magma density are three key factors which can influence the crystal size of dexamethasone sodium phosphate product.

NOMENCLATURE

a, b, c	parameters of growth rate models
B^0	nucleation rate, no·s^{-1}·m^{-3}
ΔC	supersaturation, kg·m^{-3}
G	linear growth rate, m·s^{-1}
G_m, G_1	the limiting growth rates of large crystals, m·s^{-1}
G_0	zero-size crystal growth rate, m·s^{-1}
L	crystal size, m
M_T	magma density, kg·m^{-3}
$n(L)$	population density, no·m^{-1}·m^{-3}
n^0	population density of crystal nuclei, no·m^{-1}·m^{-3}
T	absolute temperature, K
τ	mean residence time, s

REFERENCES

1 Wang, J.K., Liu, Y., "Semi-batch crystallization of 7-amino-desacetoxycephalos-pornanic", *Chinese J. Chem. Eng.*, **11** (4), 399—402 (2003).

2 Chen, H.P., "Crystallization thermodynamics and kinetics behavior of vitamin C in batch crystallizer", *Chinese J Chem. Eng.*, **8** (2), 95—99(2000).

3 Wang, J.K., Liu, Y., Yin, Q.X., "Studies on the mechanism of primary nucleation of ciprofloxacin hydrochloride monohydrate", *Chinese J. Chem. Eng.*, **10** (4), 375—380 (2002).

4 Isopescu, R., Mocioi, M., Zahanagiu, F., Filipescu, L., "Growth rate models and kinetics estimation for $CaCO_3$ precipitated in continuous crystallization", *J. Crystal Growth*, **167**, 260 (1996).

5 Randolph, A.D., Larson, M.A., Theory of Particulate Processes, Academic Press, New York (1988).

6 Mullin, J.W., Crystallization, Butterworths-Heinemann, Oxford (2000).

7 Bransom, S.H., "Factors in the design of Continuous crystallizer", *Br. Chem. Eng.*, **5**, 838—843 (1960).

8 Canning, T.F., Randolph, A.D., "Some aspects of crystallization theory: System that violate McCabe's ΔL laws", *AIChE J.*, **13**, 5—11 (1967).

9 Mydlarz, J., Jones, A.G., "On modeling the size-dependent growth rate of potassium sulphate in an MSMPR crystallizer", *Chem. Eng. Commun.*, **90**, 47—56 (1990).

10 Abegg, C.F., Stevens, J.D., Larson, M.A., "Crystal size distribution in continuous crystallizer when growth rate is size-dependent", *AIChE J.*, **14**, 188—193 (1968).

11 Rojkowski, Z., "A new empirical kinetics equation of size-dependent crystal growth and its use", *Krist. Tech.*, **12**, 1121—1126 (1977).

12 Rojkowski, Z., "Two parameter kinetic equation of size dependent crystal growth", *Krist. Tech.*, **13**, 1277—1293 (1978).

13 Mydlarz, J., Jones, A.G., "On the estimation of size-dependent crystal growth rate functions in MSMPR crystallizers", *The Chemical Engineering Journal*, **53**, 125—135 (1993).

14 Mydlarz, J., Jones, A.G., "An assessment of MSMPR crystallization kinetics data for systems modeled by size-dependent crystal growth rate functions", *The Chemical Engineering Journal*, **55**, 69—80 (1994).